Extraordinary negative thermal expansion of two-dimensional nitrides : a comparative ab initio study of quasiharmonic approximation and molecular dynamics simulations

Extraordinary negative thermal expansion of two-dimensional nitrides: A comparative ab initio study of quasi-harmonic approximation and molecular dynamics simulations

Ilker Demiroglu[1] and Cem Sevik[2]
[1] *Department of Advanced Technologies, Eskisehir Technical University, Eskisehir, TR 26555, Turkey*
e-mail address: ilkerdemiroglu@eskisehir.edu.tr
[2]*Department of Mechanical Engineering, Eskişehir Technical University, Eskisehir, TR 26555, Turkey*
e-mail address: csevik@eskisehir.edu.tr

Thermal expansion behavior of two-dimensional nitrides and graphene are studied by ab-initio molecular dynamics simulations as well as quasi harmonic approximation. Anharmonicity of the acoustic phonon modes are related with the unusual negative thermal expansion behavior of the nitrides. Our results also hint direct ab-initio molecular dynamics simulations are a more elaborate method to investigate thermal expansion behavior of two-dimensional materials than the quasi-harmonic approximation. Nevertheless, giant negative thermal expansion coefficients are found for *h*-GaN and *h*-AlN within the covered temperature range 100-600 K regardless of the chosen computational method. This unusual negative thermal expansion of two-dimensional nitrides is reasoned with the out of plane oscillations related rippling behavior of the monolayers.

Keywords: molecular dynamics, graphene, boron nitride, gallium nitride, aluminum nitride, negative thermal expansion
PACS: 65.40.De, 65.80.Ck, 82.20.Wt, 31.15.E−, 31.15.Qg, 82.45.Mp

After the discovery of graphene [1] and such novel two-dimensional (2D) nanomaterials with extraordinary properties [2,3] that will help to miniaturize further technological devices with even higher efficiency than their predecessors, a new route (forming heterostructures) emerged to mix and match the members of these materials family to further improve and adjust their properties. [3,4] In that sense, thermal properties of these nanomaterials are becoming even more critical for the performance, reliability, longevity and safety of the future device technology. Thermal expansion properties are particularly important because at working temperatures, the accumulated thermal strain and stress may influence or even destroy the device performance.

In particular, materials with negative thermal expansion (NTE) properties among the newly emerging 2D materials family particularly important as compromising thermal expansion by NTE materials is a convenient way to eliminate the aforementioned thermal expansion problems [5,6]. Very recently, it has been also shown that strain engineering via thermal expansion mismatch is an elaborate growth method for 2D materials [7] and it is shown that strain engineered heterostructures exhibit superior ion battery performances [8]. To promote a wide range of device applications, it has been long desired to develop materials with larger NTE over a wide temperature range. On the other hand, even for bulk materials, only a very limited number of NTE materials can serve as thermal expansion compensators in practice, due to the relatively narrow NTE operation-temperature window, low NTE coefficient, thermal expansion anisotropy, as well as low mechanical and/or electrical insulating properties. [9] However, as a result of a recent experiment, negative thermal expansion behavior for monolayer to trilayer *h*-BN at 300 to 400 K temperatures is presented. [10]

As the pioneer of 2D materials, thermal expansion property of graphene is studied more predominantly among other materials. Although NTE behavior is observed in general for lower temperatures, both experimental [11–18] and theoretical [19,20,29–33,21–28] results are very diverse and, in some cases, contradictory. For example, the experimental room temperature (RT) thermal expansion coefficients range from -21.4×10^{-6} K^{-1} [11] to -5.5×10^{-6} K^{-1} [12] and while some studies report a sharp increase [13,14] and a sign change to positive at around 350K [13–15], others state more horizontal behavior and no sign change up to 1000K [12,16]. In theoretical studies, on the other hand, thermal expansion values range from -10×10^{-6} K^{-1} [19] to positive values [20] at RT while they show different behaviors with respect to temperature due to the selected approach and the level of theory. This diversity is related to the importance of anharmonicities and rippling. [34] Moreover, even for the same method calculations within conventional quasi-harmonic approach, the room temperature values vary between -3.5×10^{-6} K^{-1} [21] to -1×10^{-6} K^{-1} [22], which is most probably due to the selected volume range and the existence of negative frequency phonons for the compressed models [23].

In general, direct experimental measurement of thermal expansion coefficient of 2D materials is a rough task and

usually dependent to simulations due to (I) the unwanted substrate effects which usually dominate the thermal expansion behavior and (II) the transparency of 2D materials which makes conventional optical approaches difficult. [35] Therefore, accurate theoretical procedures for the determination of thermal expansion coefficients of 2D materials are indispensable. As the NTE behavior typically originates from the presence of low-energy anharmonic vibrations of atoms, [36] quasi-harmonic approach is likely to miss the full extent of the phenomenon. On the other hand, Molecular dynamics is an elaborate method which incorporates full anharmonic interactions. However, its required large simulation system sizes to simulate thermal expansion behavior is usually a limiting factor for more accurate quantum level calculations and therefore it is studied more predominantly by various classical interaction potentials up to date. [20,31–33] In this respect, we investigate thermal expansion coefficients of graphene, *h*-BN, *h*-GaN and *h*-AlN monolayers directly by *ab-initio* molecular dynamics (MD) simulations as well as quasi-harmonic approximation (QHA) and gruneisen framework. To our knowledge there is a lack of thermal expansion studies on monolayer GaN and AlN apart from one QHA study on *h*-GaN [37] stating NTE behavior only below RT with a maximum value of -8×10^{-6} K^{-1} at 70K.

All simulations are performed by using Density functional theory (DFT) within the Vienna ab initio simulation package (VASP) [38,39]. Local density approximation [40] and projector augmented wave [41,42] methods are used together with 500 eV plane wave basis cutoff-energy. For the vibrational frequency calculations plane wave basis cutoff is increased to 700 eV. The vibrational frequencies were acquired by using PHONOPY code [43] , which can directly use the force constants obtained by density functional perturbation theory [44] provided by the VASP code. Here, 7×7×1 conventional supercell structures and 5×5×1 Γ centered k-points grids were considered for all systems. Isothermal-isobaric (NPT) [45,46] ensemble have been selected for *ab-initio* molecular dynamics [47,48] (MD) simulations. We only applied the constant pressure algorithm to the two lattice vectors parallel to the 2D plane, leaving the third vector unchanged during the simulation. MD simulations are carried for a set of constant temperatures ranging from 50K to 600 K. At each temperature, all *ab-initio* MD simulations lasted at least 8 ps with a time step of 1 fs. The friction coefficients of atomic and lattice degrees of freedom is set to 5 ps^{-1} and the external pressure is kept at 0 Pa.

To estimate thermal expansion coefficient from QHA, all phonon frequencies of relaxed systems are calculated together with compressed and strained systems. Figure 1 shows phonon dispersion relations of graphene as an example. Although no negative frequencies exist for relaxed and strained configurations, imaginary frequencies exist for the first mode close to Γ point in all the compressed configurations starting from 0.25% compression. As imaginary frequencies are not valid in QHA, we fitted vibrational frequencies of the compressed systems according to the linear relation obtained from the strained phonons to overcome the imaginary frequency problem. The fitted phonon frequencies correct the negative frequencies of the first mode while the rest of the vibrational modes match very accurately with the existing ones. The same procedure is also applied to *h*-BN, *h*-AlN and *h*-GaN systems and very similar result are obtained.

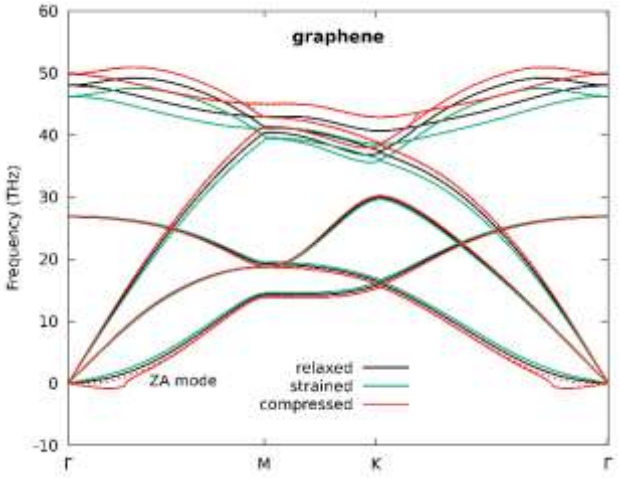

Figure 1. Phonon dispersion relations of relaxed, 1% strained and 1% compressed graphene monolayers. Dashed line shows the corrected phonon curves of the compressed case.

When the non-corrected phonons, which has negative phonon frequencies, are used in QHA, thermal expansion values underestimate significantly. For *h*-GaN the position of the minimum and the general shape matches well with the previous QHA study [37]. For graphene and *h*-BN thermal expansion values becomes positive at around 350 K and 400 K respectively while for *h*-AlN and *h*-GaN they become positive just before RT. On the other hand, with the corrected phonons, thermal expansion values are negative for all systems in the covered temperature range 100-600 K. The NTE behavior is found to be giant for *h*-GaN and *h*-AlN with very similar values around -20×10^{-6} K^{-1} at RT. For *h*-BN it is estimated around -10×10^{-6} K^{-1} at RT while for graphene it is around -6×10^{-6} K^{-1}.

Thermal expansion (α) can be also obtained by gruneisen framework approach by calculating mode-dependent gruneisen parameters ($\gamma_{q,j}$)

$$\gamma_{q,j} = -\frac{a_0}{\omega_{q,j}} \frac{\partial \omega_{q,j}}{\partial a} \quad (1)$$

and the mean gruneisen parameter (γ_{mean})

$$\gamma_{mean} \equiv \frac{\sum_{q,j} \gamma_{q,j} c_{q,j}}{\sum_{q,j} c_{q,j}} \quad (2)$$

as

$$\alpha = \frac{\gamma_{mean} C^V}{B_T V_0}\Big|_{a,T} \quad (3)$$

where a_0 is the unit cell constant, $\omega_{q,j}$ is the vibrational frequency corresponding to wave vector q and mode j, $c_{q,j}$ is the mode specific heat, C^V is the heat capacity, B_T is the bulk modulus. We calculated thermal expansion coefficient by considering 0.25% strained systems as the phonon behavior deviates from linearity with the increasing strain. Figure 2 shows that the thermal expansion behavior from gruneisen framework and from corrected QHA are the same while the absolute values of gruneisen framework are slightly larger than QHA in magnitude.

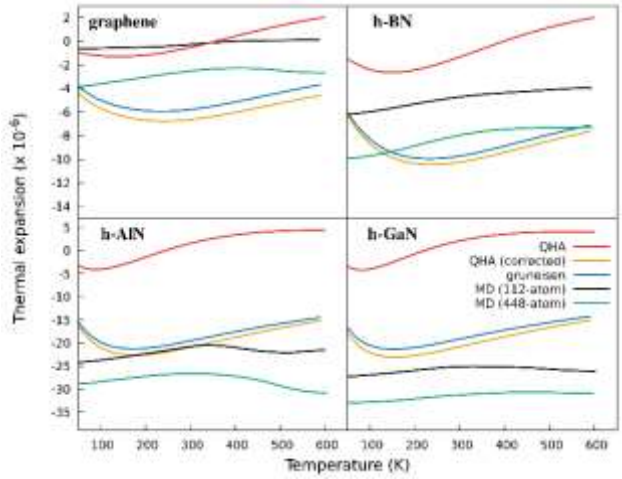

Figure 2. Calculated thermal expansion coefficients of graphene and 2D nitrides by MD simulations, QHA and gruneisen framework.

Strong anharmonicity of lattice vibrations are expected generally for 2D materials and it is argued that anharmonicity is fundamental for their stability. In the case of graphene, for example, the anharmonic coupling between bending and stretching modes, which are decoupled in harmonic approximation, can stabilize the flat phases by suppressing the long-wavelength fluctuations. [49–51] As given in equation (1), mode gruneisen parameters are basically strain dependence of phonon frequencies, and they are often used as a heuristic method to quantify anharmonicity. Mode Gruneisen parameters calculated over full mesh are given in Figure 3 for all considered 2D systems. The ZA branch (the out of plane vibration) is the main negative contributor in all four system, while the optic branches are condensed around 0. For *h*-AlN and especially for *h*-GaN the other acoustic branches also start to contribute negative mean, which indicate stronger anharmonicity for these materials and it is also reflected in their stronger NTE behavior.

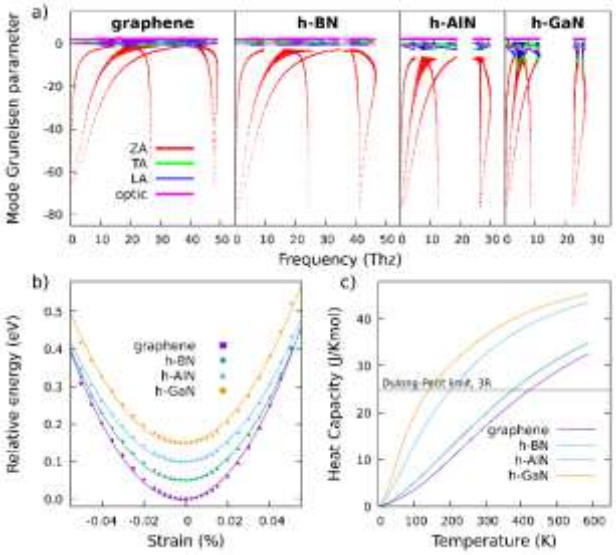

Figure 3. Calculated (a) mode gruneisen parameters, (b) energy versus strain curves and (c) heat capacity versus temperature curves (c) for graphene and 2D nitrides.

Potential energy change due to the strain can also hint phonon anharmonicity from another point of view. Here, the strain is defined by the change of lattice constant divided by its relaxed value, $[(a-a_0)/a_0]$. The potential energy wells (given in Figure 3) obtained from strained and compressed systems with respect to the positive and negative atomic displacements are found strongly asymmetric and thus deviate from harmonic behaviour. The cubic terms of the polynomial fitting quantifies the order of the anharmonicity as −421, −357, −332, and −317 meV Å^{-3} for *h*-GaN, graphene, *h*-AlN, and *h*-BN, respectively. The values for *h*-GaN and graphene are in good agreement with the results of a previous study. [52] This anharmonicity consideration is also in line with the MD simulations where the bondlength distribution around the equilibrium shows an asymmetry from harmonic behavior and more states are found for larger distances than the smaller ones (see Figure 5a in the next part as an example for *h*-GaN).

Another indication of the strong anharmonicity is the increase of specific heat beyond the Dulong–Petit limit (see Figure 3 inset). The heat capacity values obtained from QHA exceeds the Dulong–Petit limit even before 200 K for *h*-GaN and *h*-AlN and increases with the increasing temperature. The order is found as *h*-GaN > *h*-AlN > *h*-BN > graphene. The heat capacity values obtained from ab-initio molecular dynamics simulations, on the other hand, shows a constant behaviour within the temperature range (100-600 K) as in the case of a previous monte carlo study on graphene [27] but sits above Dulong–Petit limit with very similar values around 25.2 Jmol^{-1}K^{-1} for all four systems. All in all, the perceived anharmonicity order matches well with the order in thermal expansion coefficients in general as the anharmonicity is the main driving force for the NTE behaviour in 2D materials. [36]

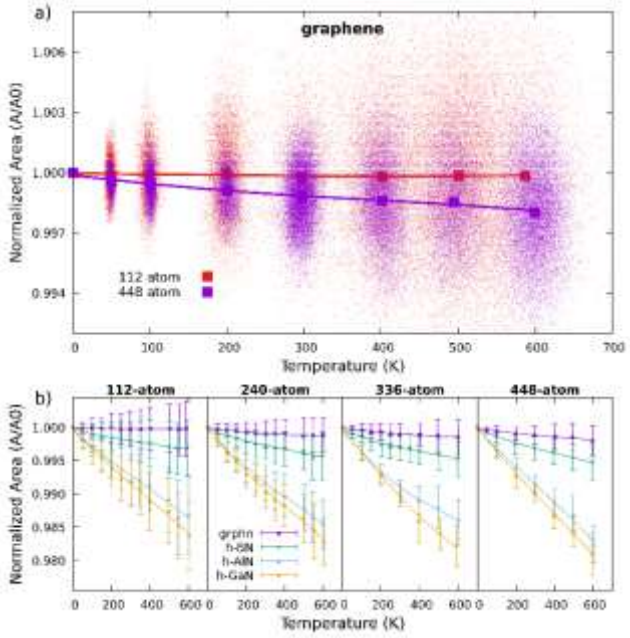

Figure 4. Normalized Area versus simulation temperature for molecular dynamics calculations. The data values of each MD frame are shown in the top graph (a), while the standard deviation is given in the bottom graphs (b) for each size.

To include the full anharmanic effects into the consideration of the thermal exansion behaviour, *ab-initio* MD simulations are conducted directly at DFT level. As the rippling effects are very important in the NTE behaviour of 2D materials, size of the system under the periodic boundary conditions becomes significant and should be treated carefully. Thus, also considering the limits of the DFT type quantum mechanical calculations, we constructed four different system sizes containing 112, 240, 336, and 448 atoms inside rectangular unit cells in the *xy* plane. Most drastic difference is found for the graphene system, for which the smallest system size the area of the cell almost does not change with increasing temperature and therefore underestimates the thermal expansion significantly (see Figure 4). For 2D nitrides, differences are smaller and the results seems to converge as the system size increases up to 448 atom (see Figure 4). The normalized area values decrease for each material with the increasing temperature as expected, and the decrease order in magnitude follow the same anharmonicity order between four considered materials: *h*-GaN > *h*-AlN > *h*-BN > graphene. However, the radial distribution function analyses shows that the bondlenths increase linearly with the increasing temperature for each system and seems independent from the system size. On the other hand, variation on the atom positions on *z* axis is effected by the system size, as the smaller unit cells do not allow full extent of the rippling behaviour (do not excite long wavelegth out of plane vibrations, in particular ZA mode). Therefore the calculated thermal expansion coefficients are found always lower in magnitude for smaller system sizes.

Figure 5 shows explicitly how the bondlengths and the rippling behaviours change with respect to temperature in 448 atom *h*-GaN system and the information for the other system sizes and other materials are given in terms of rippling width (width in *z* axis) and normalized bondlenths (d_T/d_0). These results clearly depict that the observed decrease in the area is solely due to the rippling effects which is the result of out of plane vibrations (ZA mode).

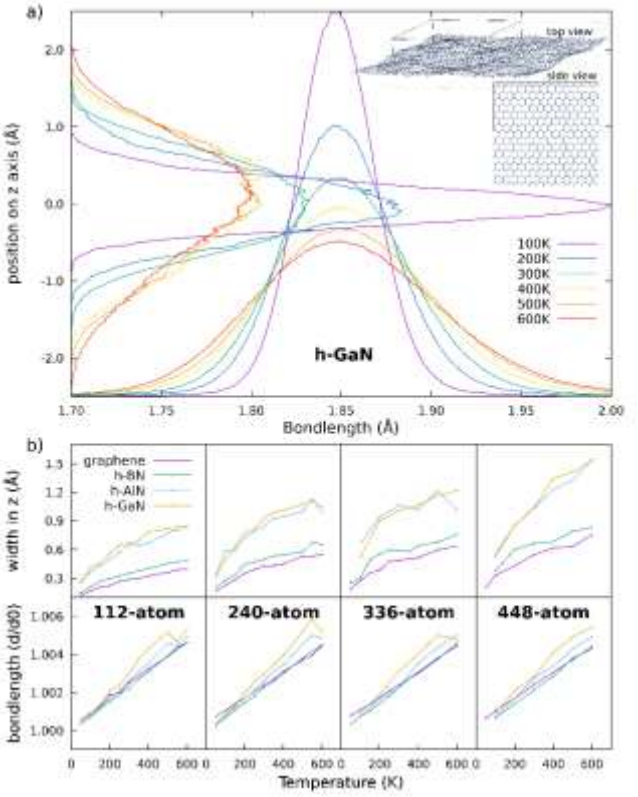

Figure 5. (a) Statistical structural analysis of 448 atom h-GaN obtained from MD simulations. The bondlength distribution is given in horizontal axis while the position distribution on z-axis is given in vertical axis. Insets show the top and side view of a MD time frame. (b) Normalized bondlengths versus temperature and rippling width versus temperature graphs of graphene and 2D nitrides obtained from MD simulations.

The rippling behaviour is found largest for *h*-GaN and *h*-AlN which causes the giant NTE behaviour for these 2D materials. In general, the order of the rippling behaviour also follows the order of the thermal expansion behaviour: *h*-GaN > *h*-AlN > *h*-BN > graphene. Previous studies also reports that the NTE behaviour in graphene is mainly from rippling and our study confirms that this behaviour is general for 2D nitrides. Thermal expansion values around RT are found as -31×10^{-6} K^{-1}, -27×10^{-6} K^{-1}, -7×10^{-6} K^{-1}, and -2.5×10^{-6} K^{-1} for *h*-GaN, *h*-AlN, *h*-BN, and graphene, respectively, from the *ab-initio* MD simulations by taking the base as the largest 448 atom systems. The RT thermal

expansion value of -7×10^{-6} K^{-1} for *h*-BN is also in very good agreement with the results of path integral monte carlo and self consistent phonon method calculations which considers nuclear quantum effects by Calvo et al. [53]. One should note that the NTE values of *h*-GaN and *h*-AlN are gigantic, which deserves scientific interest as giant NTE materials are rare and could be taken adventage from a technological point of view. Thus, experimental confirmation of the giant NTE behaviour of *h*-GaN and *h*-AlN should take precedence in 2D materials research.

When we compare the thermal expansion values obtained from the MD simulations and from the QHA, it can be seen that the NTE bahaviour is overestimated by QHA in the cases for graphene and *h*-BN while underestimates for *h*-AlN and *h*-GaN, and thus the absolute differences between QHA and MD methods hint a reverse trend for the thermal expansion behaviour with respect to the anharmonicity order. This trend is also in line with the expected trend that the stronger NTE behaviour for 2D materials with increasing anharmonicity, which hints that the MD method captures the phenomenon more complete than QHA in terms of anharmonicity. When we compare our thermal expansion values for *h*-BN with another theoretical study involving nuclear quantum effects, we can conclude that MD results are in quite good agreement

To sum up, in this study we investigated the NTE behavior of graphene and 2D nitrides by ab-initio MD and QHA methods. Our results clearly demonstrate that regardless of the calculation method *h*-GaN and *h*-AlN have giant negative thermal expansion coefficients, while the *h*-BN system has also much larger NTE behavior than graphene. The anharmonicity considerations are found consistent with the NTE behavior and the main contribution is found from the low energy acoustic phonons. Statistical analysis from the ab-initio MD simulations reveal that the bondlength increases by the temperature for all the temperature range considered and thus the NTE behavior for 2D nitrides is solely from the rippling behavior structurally.

ACKNOWLEDGEMENTS

Computational resources were provided by the High Performance and Grid Computing Center (TRGrid e-Infrastructure) of TUBITAK ULAKBIM and the National Center for High Performance Computing (UHeM) of Istanbul Technical University.

REFERENCES

[1] K. S. Novoselov, A. K. Geim, S. V Morozov, D. Jiang, Y. Zhang, S. V Dubonos, I. V Grigorieva, and A. A. Firsov, Science **306**, 666 (2004).

[2] R. Mas-Ballesté, C. Gómez-Navarro, J. Gómez-Herrero, and F. Zamora, Nanoscale **3**, 20 (2011).

[3] K. S. Novoselov, A. Mishchenko, A. Carvalho, and A. H. Castro Neto, Science (80-.). **353**, (2016).

[4] A. K. Geim and I. V. Grigorieva, Nature **499**, 419 (2013).

[5] K. Takenaka, Sci. Technol. Adv. Mater. **13**, (2012).

[6] Q. Wang, J. A. Jackson, Q. Ge, J. B. Hopkins, C. M. Spadaccini, and N. X. Fang, Phys. Rev. Lett. **117**, 175901 (2016).

[7] G. H. Ahn, M. Amani, H. Rasool, D. H. Lien, J. P. Mastandrea, J. W. Ager, M. Dubey, D. C. Chrzan, A. M. Minor, and A. Javey, Nat. Commun. **8**, 1 (2017).

[8] P. Xiong, F. Zhang, X. Zhang, S. Wang, H. Liu, B. Sun, J. Zhang, Y. Sun, R. Ma, Y. Bando, C. Zhou, Z. Liu, T. Sasaki, and G. Wang, Nat. Commun. **11**, 1 (2020).

[9] Y. Nakamura, K. Takenaka, A. Kishimoto, and H. Takagi, J. Am. Ceram. Soc. **92**, 2999 (2009).

[10] Q. Cai, D. Scullion, W. Gan, A. Falin, S. Zhang, K. Watanabe, T. Taniguchi, Y. Chen, E. J. G. Santos, and L. H. Li, Sci. Adv. **5**, eaav0129 (2019).

[11] X. Hu, P. Yasaei, J. Jokisaari, S. Öğüt, A. Salehi-Khojin, and R. F. Klie, Phys. Rev. Lett. **120**, 055902 (2018).

[12] W. Pan, J. Xiao, J. Zhu, C. Yu, G. Zhang, Z. Ni, K. Watanabe, T. Taniguchi, Y. Shi, and X. Wang, Sci. Rep. **2**, 1 (2012).

[13] C. Li, Q. Liu, X. Peng, and S. Fan, Meas. Sci. Technol. **27**, 075102 (2016).

[14] W. Bao, F. Miao, Z. Chen, H. Zhang, W. Jang, C. Dames, and C. N. Lau, Nat. Nanotechnol. **4**, 562 (2009).

[15] S. Linas, Y. Magnin, B. Poinsot, O. Boisron, G. D. Förster, V. Martinez, R. Fulcrand, F. Tournus, V. Dupuis, F. Rabilloud, L. Bardotti, Z. Han, D. Kalita, V. Bouchiat, and F. Calvo, Phys. Rev. B - Condens. Matter Mater. Phys. **91**, 075426 (2015).

[16] D. Yoon, Y. W. Son, and H. Cheong, Nano Lett. **11**, 3227 (2011).

[17] G. López-Polín, M. Ortega, J. G. Vilhena, I. Alda, J. Gomez-Herrero, P. A. Serena, C. Gomez-Navarro, and R. Pérez, Carbon N. Y. **116**, 670 (2017).

[18] V. Singh, S. Sengupta, H. S. Solanki, R. Dhall, A. Allain, S. Dhara, P. Pant, and M. M. Deshmukh, Nanotechnology **21**, (2010).

[19] V. N. Bondarev, V. M. Adamyan, and V. V. Zavalniuk, Phys. Rev. B **97**, 035426 (2018).

[20] H. Ghasemi and A. Rajabpour, in *J. Phys. Conf. Ser.* (2017).

[21] N. Mounet and N. Marzari, Phys. Rev. B - Condens. Matter Mater. Phys. **71**, 205214 (2005).

[22] T. Shao, B. Wen, R. Melnik, S. Yao, Y. Kawazoe, and Y. Tian, J. Chem. Phys. **137**, 194901 (2012).

[23] X. J. Ge, K. L. Yao, and J. T. Lü, Phys. Rev. B **94**, 165433 (2016).

[24] S. Mann, P. Rani, R. Kumar, and V. K. Jindal, in *AIP Conf. Proc.* (American Institute of Physics Inc., 2016), p. 110038.

[25] S. Mann, R. Kumar, and V. K. Jindal, RSC Adv. **7**, 22378 (2017).
[26] C. Sevik, Phys. Rev. B - Condens. Matter Mater. Phys. **89**, 035422 (2014).
[27] K. V. Zakharchenko, M. I. Katsnelson, and A. Fasolino, Phys. Rev. Lett. **102**, 046808 (2009).
[28] J. W. Jiang, J. S. Wang, and B. Li, Phys. Rev. B - Condens. Matter Mater. Phys. **80**, 205429 (2009).
[29] E. Madenci, A. Barut, and M. Dorduncu, in *Proc. - Electron. Components Technol. Conf.* (Institute of Electrical and Electronics Engineers Inc., 2019), pp. 825–833.
[30] M. Pozzo, D. Alfè, P. Lacovig, P. Hofmann, S. Lizzit, and A. Baraldi, Phys. Rev. Lett. **106**, (2011).
[31] W. Gao and R. Huang, J. Mech. Phys. Solids **66**, 42 (2014).
[32] Alamusi, H. Li, Y. Ning, B. Gu, N. Hu, W. Yuan, F. Jia, H. Liu, Y. Li, Y. Liu, H. Ning, L. Wu, S. Fu, and Y. Cai, Mol. Simul. **44**, 34 (2018).
[33] C. P. Herrero and R. Ramírez, J. Chem. Phys. **148**, 102302 (2018).
[34] A. Fasolino, J. H. Los, and M. I. Katsnelson, Nat. Mater. **6**, 858 (2007).
[35] L. Zhang, Z. Lu, Y. Song, L. Zhao, B. Bhatia, K. R. Bagnall, and E. N. Wang, Nano Lett. **19**, 4745 (2019).
[36] R. Mittal, M. K. Gupta, and S. L. Chaplot, Prog. Mater. Sci. **92**, 360 (2018).
[37] G. Qin, Z. Qin, H. Wang, and M. Hu, Phys. Rev. B **95**, 195416 (2017).
[38] G. Kresse and J. Hafner, Phys. Rev. B **47**, 558 (1993).
[39] G. Kresse and J. Hafner, Phys. Rev. B **49**, 14251 (1994).
[40] J. P. Perdew and A. Zunger, Phys. Rev. B **23**, 5048 (1981).
[41] G. Kresse and D. Joubert, Phys. Rev. B **59**, 1758 (1999).
[42] P. E. Blöchl, Phys. Rev. B **50**, 17953 (1994).
[43] A. Togo, F. Oba, and I. Tanaka, Phys. Rev. B **78**, 134106 (2008).
[44] S. Baroni, S. De Gironcoli, A. Dal Corso, and P. Giannozzi, Rev. Mod. Phys. **73**, 515 (2001).
[45] E. Hernández, J. Chem. Phys. **115**, 10282 (2001).
[46] *Computer Simulation of Liquids: Second Edition - Michael P. Allen, Dominic J. Tildesley - Google Kitaplar* (n.d.).
[47] M. Parrinello and A. Rahman, J. Appl. Phys. **52**, 7182 (1981).
[48] M. Parrinello and A. Rahman, Phys. Rev. Lett. **45**, 1196 (1980).
[49] K. V. Zakharchenko, M. I. Katsnelson, and A. Fasolino, Phys. Rev. Lett. **102**, 046808 (2009).
[50] A. L. C. Da Silva, L. Cândido, J. N. Teixeira Rabelo, G. Q. Hai, and F. M. Peeters, EPL **107**, 56004 (2014).
[51] A. Fasolino, J. H. Los, and M. I. Katsnelson, Nat. Mater. **6**, 858 (2007).
[52] Z. Qin, G. Qin, X. Zuo, Z. Xiong, and M. Hu, Nanoscale **9**, 4295 (2017).
[53] F. Calvo and Y. Magnin, Eur. Phys. J. B **89**, 1 (2016).